Chapter 4
Determination of Dynamic Interlayer Strength Properties of Layered Composites Using Measuring Bars

Artem V. Basalin, Anatoly M. Bragov, and Aleksandr Yu. Konstantinov

Abstract The paper presents the results of the development and testing of experimental schemes that allow us to study the characteristics of the interlayer strength of layered composite materials. The schemes are based on the technique of measuring bars. To determine the interlayer strength at separation, a modification of the Kolsky method for direct tension is used. A sample of a special shape is glued to adapters having threaded parts, by means of which the sample is installed in a split measuring bar. To determine the mechanical characteristics of composite materials during interlayer shear, three experimental schemes were proposed and tested: dynamic three-point bending of a short beam, dynamic compression of plate samples with incisions and dynamic extrusion of the middle part of the samples in the form of parallelepipeds. Loading of samples and registration of their deformation processes were carried out using the technique of measuring bars. A numerical simulation was carried out to check the dynamic equilibrium condition of the sample in an experiment on the dynamic bending of a short beam. The schemes were tested on samples of a layered composite material with a polymer matrix reinforced with carbon fabric. The results of a comparative analysis of the schemes for determining shear strength showed that the most preferable is the scheme of extrusion of the middle part of the parallelepiped, since, unlike the bending of the beam, it allows you to vary and control the loading conditions, and unlike the testing of incised samples, it is symmetrical, which eliminates the appearance of bending moments in the sample.

A. V. Basalin · A. M. Bragov · A. Yu. Konstantinov (✉)
National Research Lobachevsky State University of Nizhny Novgorod, Gagarin Ave. 23, Nizhni Novgorod, Russia 603022
e-mail: konstantinov@mech.unn.ru

A. V. Basalin
e-mail: basalin@mech.unn.ru

A. M. Bragov
e-mail: bragov@mech.unn.ru

4.1   Introduction

The structures made of multilayer composite materials based on glass or carbon fiber and plastic binder (polymer composite materials or PCM) during exploitation can be subjected to dynamic loads of various natures. Interest in the study of the behavior of such materials under intense dynamic loads is determined by the requests of the aerospace and automotive industries, energy technology, construction, etc. Composite materials have a set of properties and features that differ from traditional structural materials (metal alloys) and together open up wide opportunities both for improving existing structures of various purposes and for developing new structures and technological processes. To calculate stress–strain state and assess the strength of structures, modern computing systems are used, for example, ANSYS, LS-DYNA, ABAQUS, LOGOS, etc. The creation of digital models of real structural elements greatly facilitates the optimization of the design under development and significantly reduces the design time, but requires a large amount of reliable experimental information. The development of new materials and the increasing complexity of mathematical models lead to the need to develop experimental research tools. For multilayer composite materials based on glass or carbon fiber and plastic binder (polymer composite materials or PCM), the range of dynamic loads has not been studied much. Available scattered experimental data on the effect of the strain rate on the strength properties of individual classes of composites for specific loading conditions.

Currently, the methods of dynamic testing based on the classical Hopkinson-Kolsky split bar scheme have received the greatest development [14]. The main idea of the method is to use bars measuring indirectly the movement of sample points over time and the history of changes in the force acting on the sample during loading. Due to the small length of the sample compared to the length of the loading pulse, stresses and strains are evenly distributed along its entire length, and deformation occurs under conditions of so-called "dynamic equilibrium". Currently, many modifications of the Split Hopkinson Pressure Bar (SHPB) method are used for compression, tension, shear, torsion, etc. A description of various variants of SHPB can be found in Campbell and Dowling [3–5, 7–9, 12, 15, 18, 19, 21].

In the last decade, methods based on the technique of measuring bars have been widely used for the study of polymers [20] and structural PCM with various reinforcement schemes. For example, studies of the effect of the strain rate on the dynamic behavior of woven PCM under tension [10, 11] and compression [2, 16] have been carried out. The strain rate dependences of the deformation curves of unidirectional carbon fiber plastics under tension [17] and compression [13] in the direction transverse to the direction of the fibers and shear in the plane of the layer [13] are obtained at deformation rates of ~1000 1/s. Cherniaev et al. [6] obtained deformation diagrams of unidirectional carbon fiber in the direction perpendicular to the direction of the fibers in the range of strain rates 10–2000 1/s using the copra test method and the SHPB method. In Akl and Baz [1], experimental studies of the dynamic behavior and damping properties during compression of a thermoplastic polymer filled with

carbon nanoparticles using the classical scheme of the SHPB method at strain rates of 2000–7000 1/s were carried out.

The purpose of this work is to develop and test methods for studying the dynamic characteristics of the strength of layered PCM during interlayer fracture: shear and separation.

4.2 Determination of Interlayer Strength at Separation

This section describes an experimental scheme for determining the ultimate strength at the tension of the PCM in the direction perpendicular to the reinforcement plane. A sample from a special-shaped PCM is attached to measuring bars using a snap-in (Fig. 4.1). The system is loaded with a tensile pulse. In order to fix the sample in the measuring bars, special adapters are used. Centering of the sample is performed by drilling holes in the samples into which the adapter guides are inserted. The sample is connected to the adapters by means of an adhesive joint. The "sample-adapter" assembly is screwed into the measuring bars. This mounting scheme allows you to prepare several samples for testing at once, while in the case of gluing the sample directly to the measuring bars, the testing process slows down noticeably.

To determine the ultimate stress at which the fracture of the sample occurs according to the interlayer separation (perpendicular to the reinforcement plane σ_3), the following ratio is used:

$$\sigma_3^+ = max\left(\frac{E_T \cdot S_T \cdot \varepsilon^T(t)}{a^2}\right)$$

where ε^T—the transmitted strain pulse registered in the output bar, E_T, S_T—Young's modulus and cross section area of the output bar and a—sample section side.

The left part of Fig. 4.2 shows the characteristic time dependences of the tensile stress in the cross section of the sample (blue line) and the rate of tension (red dotted line). The ultimate value of the stress was determined as the maximum values of $\sigma_{3+}(t)$. At the same time, the rate of tension at the moment of fracture of the sample was determined. The data obtained during the testing of carbon fabric layered PCM
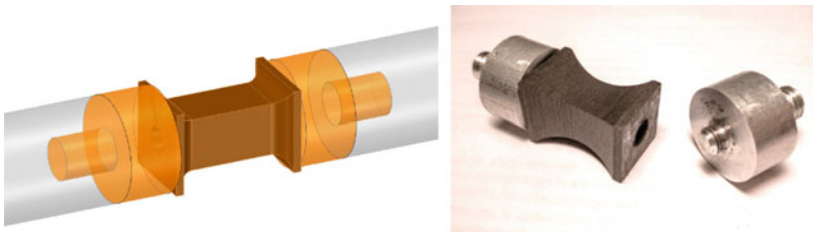
Fig. 4.1 Test scheme for determining the tensile strength of the PCM in the normal direction
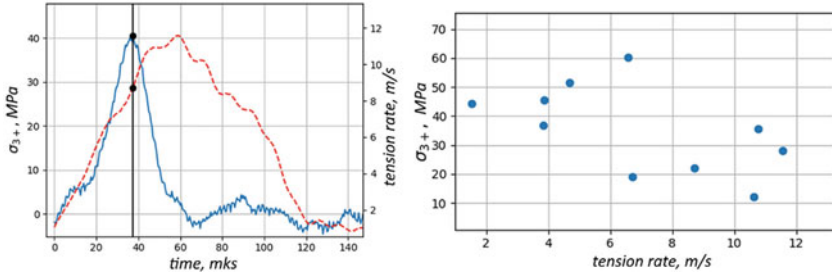
Fig. 4.2 Results of the experiment
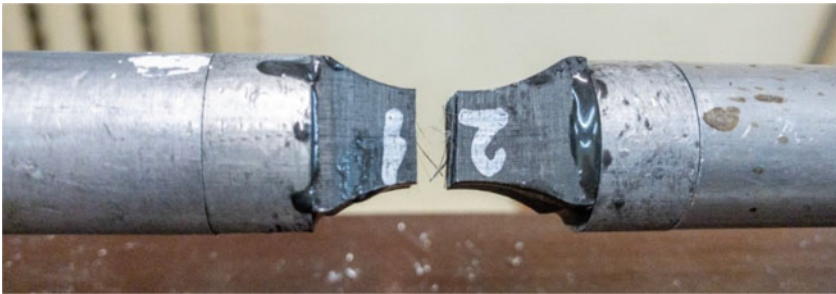
Fig. 4.3 Sample after the test

are shown in the right part of Fig. 4.2. It can be noted that the value of σ_{3+} decreases with increasing loading speed.

The sample after the test is shown in Fig. 4.3.

4.3 Determination of Interlayer Shear Strength by Bending a Short Beam

To determine the strength characteristics of the interlayer shear of the PCM under dynamic loading, by analogy with the standard for static testing of composites ISO 14130:1997, experiments were conducted on the three-point bending of a short beam. The general test scheme is illustrated in Fig. 4.4. In the experiments, measuring bars with a diameter of 20 mm were used. The radii of the rounding bars and the distance between the support bars were selected according to standard ISO 14130:1997. The geometric characteristics of the beam samples (length L, width W and height H) are shown in Fig. 4.4. The sample sizes were $45 \times 12 \times 6$ mm. A compressive pulse through a loading measuring bar loads the sample.

One of the fundamental assumptions and conditions of applicability of the Kolsky or SHPB method for determining the characteristics of materials is the condition of
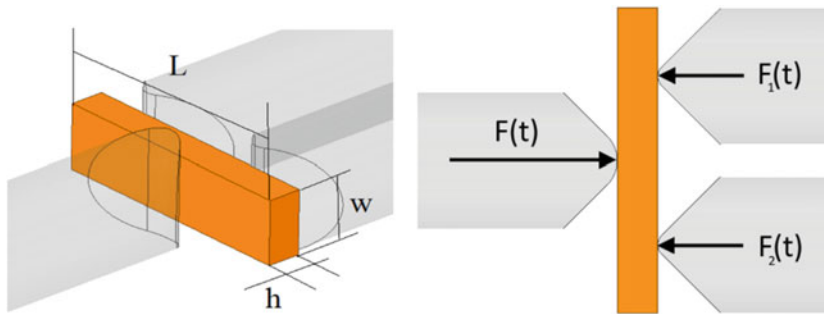
Fig. 4.4 Geometric characteristics of the sample and the forces acting on the beam during the test

dynamic equilibrium of the sample during loading. This means that at each moment of time, the force acting on the sample from the side of the loading measuring bar $F(t)$ must be equal to the sum of the forces acting on the sample from the side of the support bars $F_1(t) + F_2(t)$.

Numerical simulation was carried out to assess the conditions of dynamic equilibrium of the sample-beam in the used configuration of the test facility. The simulation was carried out in LS-DYNA code (Customer number 1069197). The results are shown in Fig. 4.5, which shows the history of changes in the forces acting on the sample from the measuring bars. The numbers indicate 1–the force from the contact "loading bar-sample", 2–the doubled force from the contact "sample-support bar" and 3–the doubled force calculated according to the data of the strain gauges on the support bar. The following conclusions can be drawn: firstly, the force acting on the sample from the side of the loading bar at each moment of time is very close in magnitude to the force acting on the sample from the side of the output-measuring bars. The time difference between the beginning of the action of the first force (F) and the appearance of the force on the support bars (F_1 and F_2) is about 10 microseconds, i.e., in the process of deformation, a dynamic equilibrium condition occurs in the sample. Secondly, the information from the strain gauge located on the support bar allows to determine accurately the force F_1 (F_2).

To process the experimental information obtained during the bending of a composite beam, the following relations are used:

The deflection rate of the beam is equal to

$$V_b(t) = c_I \cdot \left(\varepsilon^I + \varepsilon^R\right) - 0.5 \cdot c_T\left(\varepsilon_1^T + \varepsilon_2^T\right)$$

The deflection is calculated by the following formula:

$$U_b(t) = \int_0^t V_b(\tau)d\tau$$

Force acting on the beam from the input bar is calculated by the following formula:

Fig. 4.5 Forces acting on the sample: 1–force from the "loading bar-sample" contact, 2–doubled force from the "sample-support bar" contact and 3–doubled force calculated from the data of the strain gauge on the support bar
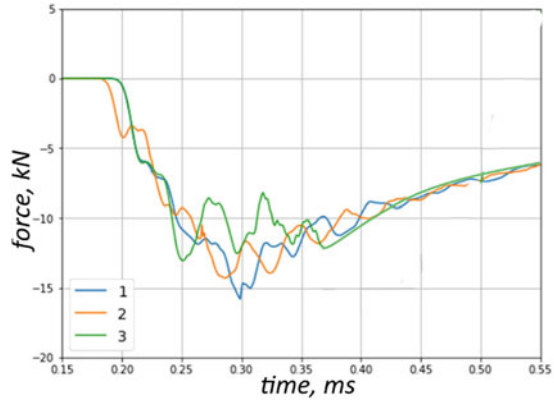
$$F(t) = F_1(t) + F_2(t) = E_T \cdot S_T \cdot \left(\varepsilon_1^T + \varepsilon_2^T\right)$$

where ε^I, ε^R—incident and reflected strain pulses measured in the input bar, ε_1^T, ε_2^T—transmitted strain pulses registered in output bars, c_I—the speed of sound of input bar's material, c_T—the speed of sound of material of output bars and E_T, S_T—Young's modulus and cross section area of output bars.

Interlayer shear stress is calculated by the following formula:

$$\tau(t) = \frac{3}{4} \cdot \frac{F(t)}{h \cdot w}$$

The ultimate interlayer shear stress is the maximum value of $\tau(t)$. . The valid tests are only those in which a single or multiple bundle was formed in the sample at the end of the beam (Fig. 4.6).

The scheme was tested on beams made of laminated PCM based on carbon fiber. Photos of the samples after the test are shown in Fig. 4.7. Depending on the amplitude of the loading wave (the velocity of the impactor), different modes of fracture of the sample are observed. On the left side of the photo, a single crack appears on the end of the sample, and on the right, there is an intense multiple delamination in the loading zone.

The characteristic strain pulses recorded in the experiment are shown in Fig. 4.8. It can be noted that the pulses recorded on the support bars are in good agreement with each other, which indicates the correct alignment of the experimental setup and the exact installation of the test sample.

single bundle   multiple bundle

Fig. 4.6 "Valid" types of fracture of the sample
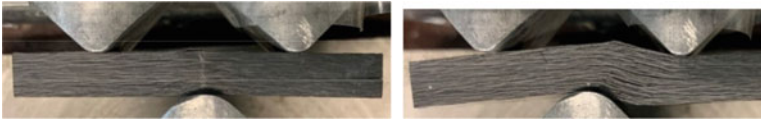
Fig. 4.7 Types of sample fracture
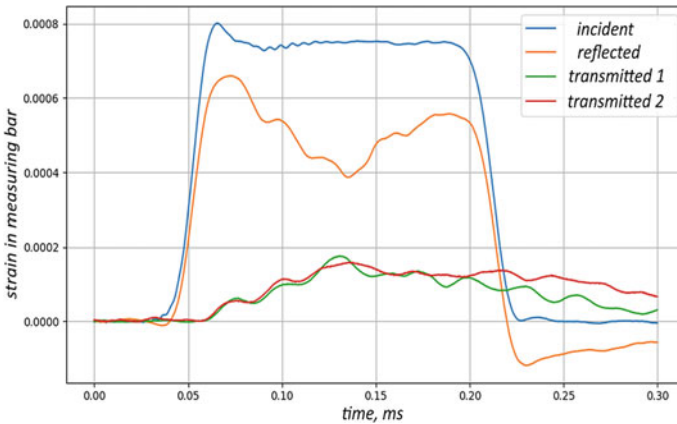
Fig. 4.8 Characteristic strain pulses recorded in the experiment for three-point bending of a short beam

Figure 4.9 illustrates a comparison of the forces acting on the sample from the loading (F) and support ($F_1 + F_2$) bars. It can be noted that these forces correspond quite well, which indicates that the conditions of dynamic equilibrium of the sample-beam during bending are met.

Based on the results of the experiment using the formulas given above, the following parameters were calculated: the deflection rate of the beam, the force F acting on the sample during the test and the magnitude of the shear stress τ. The left part of Fig. 4.10 shows the history of changes in the deflection rate of the beam (blue

Fig. 4.9 Comparison of the forces acting on the sample from the measuring bars in the bending test
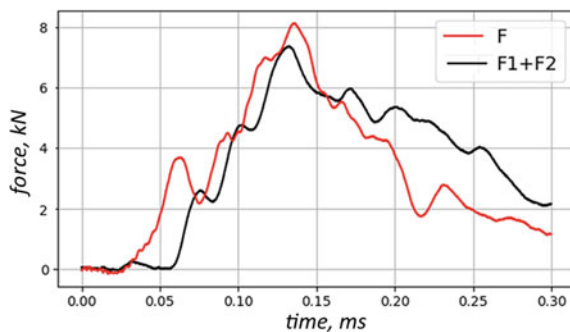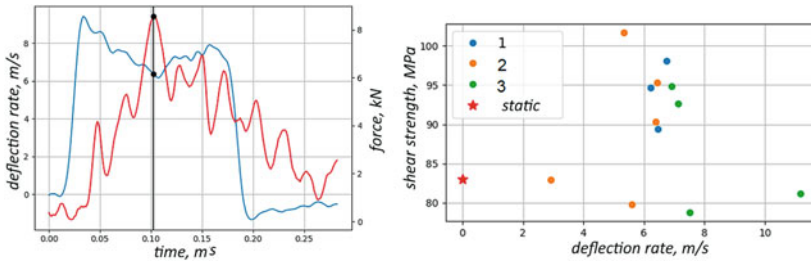
Fig. 4.10 Processing and results of the bending tests

line, left vertical axis) and the force F acting on it (red line, right vertical axis). For each experiment, the maximum value of the force and the corresponding value of the deflection velocity were determined. According to the maximum force F, using the appropriate formula, the value of the ultimate strength of the PCM during interlayer shear was calculated. The velocity dependences of the strength characteristics are presented in the right part of Fig. 4.10. The color of the dots characterizes the fracture modes of the sample: 1—corresponds to the appearance of a single crack at the end of the sample, 2—the appearance of multiple delamination at the end of the sample and 3—intense multiple delamination in the loading zone. It can be concluded that the dynamic strength is 15% higher than the static value.

4.4 Determination of Interlayer Shear Strength by Compression of Samples of Special Shape

In the second scheme, samples with incisions were tested to determine the interlayer shear strength. The configuration of the sample and equipment for fixing the sample in the measuring device is shown in Fig. 4.11.

For processing experimental information, the following relations are used:

The shear rate is equal to

$$V_{sh}(t) = c_I \cdot \left(\varepsilon^I + \varepsilon^R\right) - c_T \cdot \varepsilon^T$$
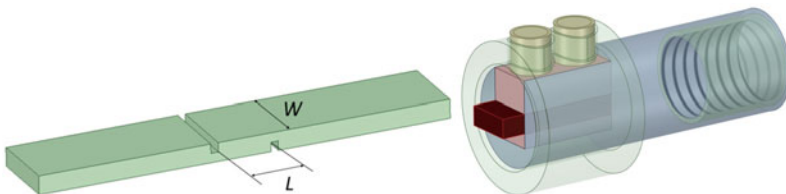
Fig. 4.11 Sample configuration for determining interlayer shear strength
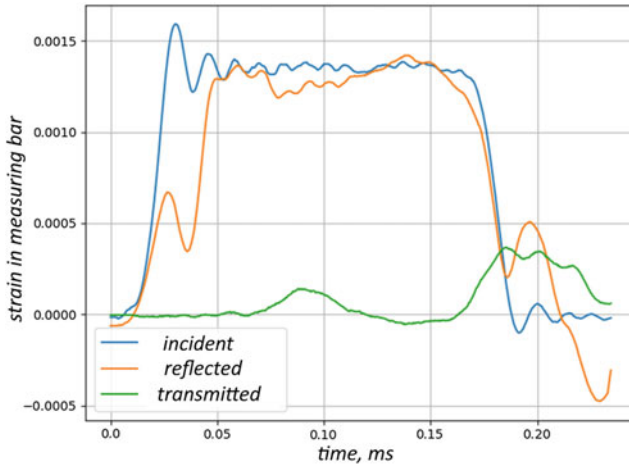
Fig. 4.12 Characteristic strain pulses recorded in the compression experiment of samples with incisions

Shear stress is calculated by the following formula:

$$\tau(t) = \frac{E_T \cdot S_T \cdot \varepsilon^T}{L \cdot w}$$

where ε^I, ε^R—incident and reflected strain pulses measured in the input bar, ε^T—transmitted strain pulse registered in output bar, c_I—the speed of sound of input bar's material, c_T—the speed of sound of material of output bars, E_T, S_T—Young's modulus and cross section area of output bars and L and W—length and width of the working area of the sample.

The scheme was tested on beams made of laminated PCM based on carbon fiber. The characteristic strain pulses recorded in the experiment are shown in Fig. 4.12.

Figure 4.13 illustrates a comparison of the forces acting on the sample from the loading (F_1) and support (F_2) bars calculated according to the Kolsky formulas. The presence of complex equipment for attaching the sample to the measuring bars (forks + tightening clips) distorts the wave pattern. Massive elements lead to additional wave reflections. A drop appears at the beginning of the reflected pulse and, accordingly, an outburst appears on the force, which is determined by the difference between the incident and reflected pulses, which does not reflect the force acting on the sample, but is a superposition of forces acting on the sample and an inert massive rigging. However, during the loading of the sample, the condition of dynamic equilibrium takes place.

Based on the results of the experiment using the formulas given earlier, the following parameters were calculated: the shear rate, the force F acting on the sample during the test and the magnitude of the shear stress τ. The left part of Fig. 4.14 shows the history of changes in the shear rate (blue line, left vertical axis) and the force

Fig. 4.13 Comparison of
the forces acting on the
sample from the measuring
bars in the shear test
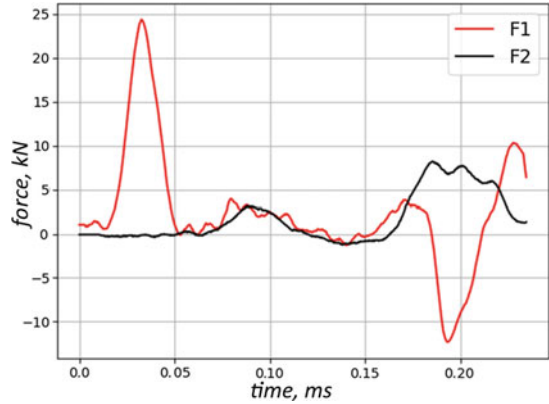
F acting on the sample (red line, right vertical axis). The stress has several peaks.
The first corresponds to the destruction of the sample along the cut plane. During
the second peak, the parts of the sample are closed when the gap formed by the cut
is estimated. For each experiment, the maximum value of the force in the first peak
and the corresponding value of the shear rate were determined. According to the
maximum force F, the value of the strength of the PCM during interlayer shear was
calculated using the appropriate formula. The velocity dependences of the strength
characteristics are presented in the right part of Fig. 4.14. The points are grouped by
the thickness of the sample. Blue markers correspond to the data obtained on samples
with a thickness of 2 mm, and orange—on samples with a thickness of 6.5 mm. The
dynamic strength according to the specified test method turned out to be lower than
the static one.
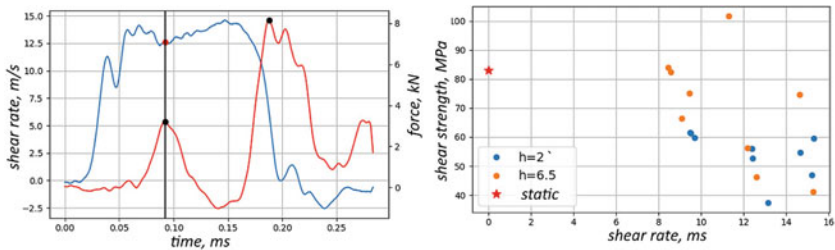
Fig. 4.14 Processing and results of the experiment on compression of samples with incisions

4.5 Determination of the Interlayer Shear Strength of the PCM by Extrusion of the Middle of the Parallelepiped Sample

To determine the interlayer shear strength of the PCM, a scheme was used to extrude the middle of the sample-parallelepiped (two-plane shift). Loading in the RSG system was carried out by a compressive load. The general view of the experimental scheme is shown in Fig. 15a. The equipment for loading sample 5 (Fig. 15b) in the SHPB system (measuring bars 1 and 2) includes parts 3 and 4, as well as a guide 6 for centering parts.

When loading the sample in the described tooling, it shifts along the planes highlighted in red in Fig. 4.16. Samples of 25 × 25x10 mm were tested.

The following relations are used to process experimental information:

Shear rate:

$$V_{sh}(t) = c_I \cdot \left(\varepsilon^I + \varepsilon^R\right) - c_T \cdot \varepsilon^T$$

Shear stress:

a   b
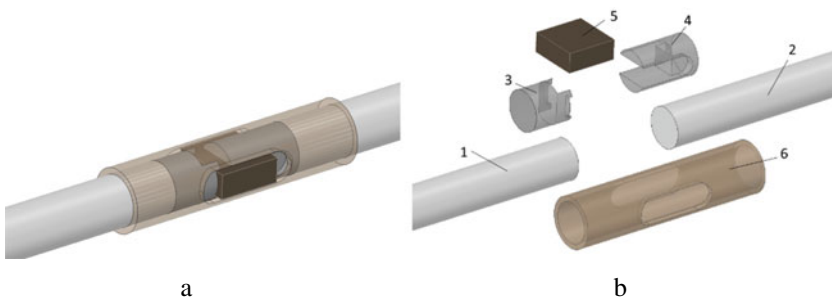
Fig. 4.15 General view of the experimental scheme

Fig. 4.16 Geometric characteristics of the sample
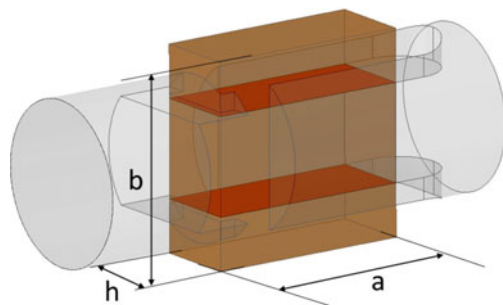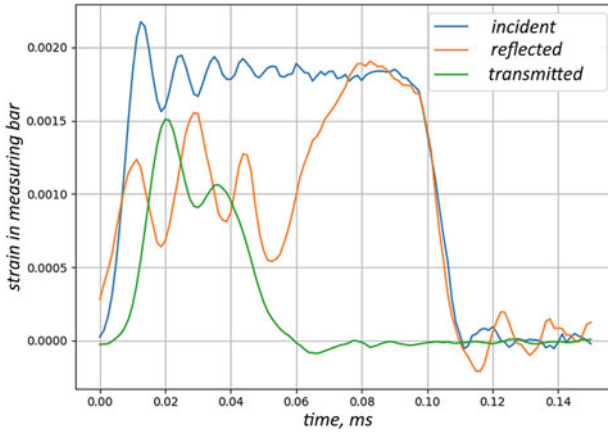
Fig. 4.17 Characteristic strain pulses recorded in the extrusion experiment

$$\tau(t) = \frac{E_T \cdot S_T \cdot \varepsilon^T}{2 \cdot a \cdot h}$$

where ε^I, ε^R—incident and reflected strain pulses measured in input bar, ε^T—transmitted strain pulse registered in output bar, c_I—the speed of sound of input bar's material, c_T—the speed of sound of material of output bars, E_T, S_T—Young's modulus and cross section area of output bars and a and h are the length and width of the shear zone.

The scheme was tested on beams made of laminated PCM based on carbon fiber. The characteristic strain pulses recorded in the experiment are shown in Fig. 4.17.

Figure 4.18 illustrates a comparison of the forces acting on the sample from the loading (F_1) and support (F_2) bars calculated according to the Kolsky formulas. It is seen that the presence of adapters used to implement extrusion introduces distortions into the wave pattern, as a result of which the conditions of dynamic equilibrium are not met.

Based on the results of the experiment, the following parameters were calculated: the shear rate, the force F acting on the sample during the test and the magnitude of the shear stress τ. The force is determined by the strain in the output-measuring bar. The left part of Fig. 4.19 shows the history of changes in the shear rate (blue line, left vertical axis) and the force F acting on the sample (red line, right vertical axis). For each experiment, the maximum value of the force and the corresponding value of the shear rate were determined. According to the maximum force F, the value of the strength of the PCM during interlayer shear was calculated using the appropriate formula. The results of processing all experiments are illustrated in the right part of Fig. 4.19. The asterisk corresponds to the static value of shear strength during interlayer shear. The values of interlayer shear strength obtained in the dynamic range were on average 25% lower than the static characteristic.
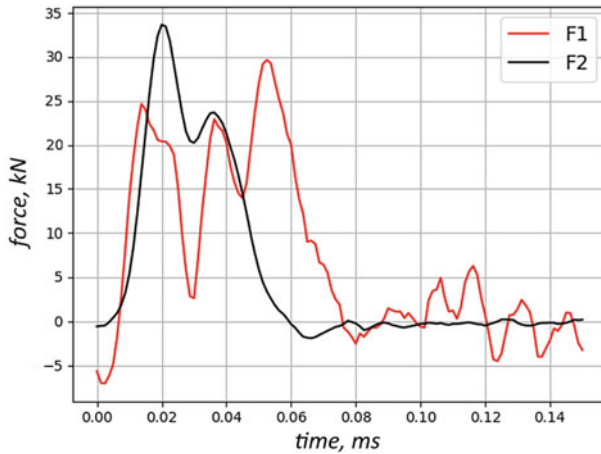
Fig. 4.18 Comparison of forces acting on the sample from the measuring rods in the extrusion experiment
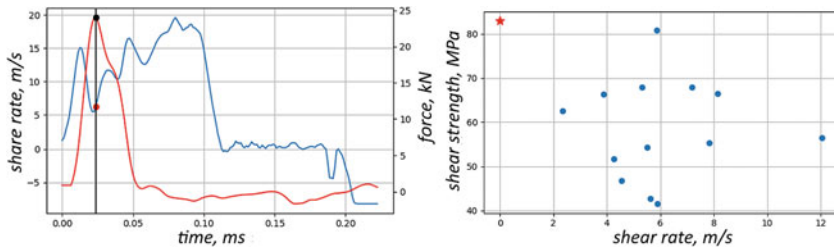
Fig. 4.19 Processing and results of the extrusion experiments

4.6   Comparative Analysis of Schemes for Interlayer Shear

Figure 4.20 shows a comparison of the values of the strength of the PCM during interlayer shear obtained by different methods. It can be noted that the data obtained by extrusion (red triangles) are in good agreement with the data determined by the dynamic compression of samples with incisions (orange and blue squares). The strength characteristic determined by the method of bending a short beam turned out to be noticeably higher.

4.7   Conclusions

As a result of the work performed, a number of experimental schemes and corresponding experimental installations were created based on the technique of
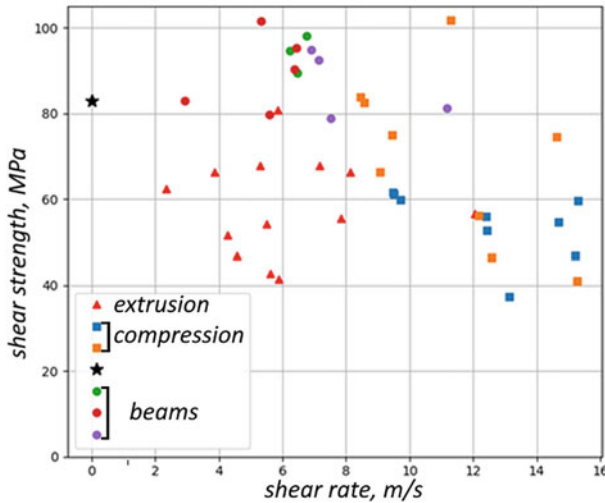
Fig. 4.20 Comparison of data obtained by different methods

measuring bars, which allow testing samples from PCM to determine the strength characteristics of interlayer shear and separation depending on the loading speed. The method of dynamic bending of a short beam does not allow varying the loading conditions in a sufficiently wide range, since the shape of the fracture of the sample changes depending on the intensity of the load. In addition, in this type of test, it is impossible to assess the conditions of destruction by the shape under study (for example, the shear rate). The scheme for testing a sample with incisions is asymmetric. Despite the small thickness of the sample, due to geometric features, a bending moment occurs, which can disrupt the isolation of the fracture mode by interlayer shear. The most informative is the scheme with the extrusion of the middle part of the sample in the form of a parallelepiped. The approbation of the schemes was carried out on the example of a layered composite of woven reinforcement. A comparative analysis of the data obtained according to the described schemes is performed.

References

1. Akl W, Baz AM (2018) Dynamic behavior and damping characteristics of carbon black polymer composites at high strain rates. Adv Polym Technol 37(2):3364–3375. https://doi.org/10.1002/ADV.22120

2. Bandaru AK, Chouhan H, Bhatnagarc N (2020) High strain rate compression testing of intraply and inter-ply hybrid thermoplastic composites reinforced with Kevlar/basalt fibers. Polymer Testing 84, Article No 106407. https://doi.org/10.1016/j.polymertesting.2020.106407.

3. Bol'shakov AP, Novikov SA, Sinitsyn VA (1979) Dynamic uniaxial tension and compression curves of copper and alloy AMg6. Strength Mater 11(10):1159–1161. https://doi.org/10.1007/BF00768612

4. Bragov AM, Gandurin VP, Grushevsky GM, Lomunov AK (1995) New potentials of Kol'skii's method for studying the dynamic properties of soft soils. J Appl Mech Tech Phys 36(3):476–481. https://doi.org/10.1007/BF02369791

5. Campbell JD, Dowling AR (1979) The behaviour of materials subjected to dynamic incremental shear loading. J Mech Phys Solids 18(1):43–63. https://doi.org/10.1016/0022-5096(70)90013-X

6. Cherniaev A, Zenga Y, Cronina D, Montesanoa J (2019) Quasi-static and dynamic characterization of unidirectional non-crimp carbon fiber fabric composites processed by HP-RTM. Polym Testing 76:65–375. https://doi.org/10.1016/J.POLYMERTESTING.2019.03.036

7. Dharan CKH, Hauser FE (1970) Determination of stress-strain characteristics at very high strain 18 rates. Exp Mech 10(9):370–376. https://doi.org/10.1007/BF02320419

8. Doerner MF, Nix WD (1986) A method for interpreting the data from depth-sensing indentation instruments. J Mater Res 1(4):601–609. https://doi.org/10.1557/JMR.1986.0601

9. Duffy JA, Campbell JD, Hawley RH (1971) On the use of a torsional split Hopkinson bar to study rate effects in 1100-0 aluminum. J Appl Mech 38(1):83–91. https://doi.org/10.1115/1.3408771

10. Elmahdy A, Verleysen P (2020) Mechanical behavior of basalt and glass textile composites at high strain rates: a comparison. Polym Test 81, Article No. 106224. DOI:https://doi.org/10.1016/j.polymertesting.2019.106224.

11. Elmahdy A, Verleysen P (2019) Tensile behavior of woven basalt fiber reinforced composites at high strain rates. Polym Test 76:207–221. https://doi.org/10.1016/j.polymertesting.2019.03.016

12. Klepaczko JR (1982) Discussion of a new experimental method in measuring fracture toughness initiation at high loading rates by stress waves. Transactions of the ASME. Journal of Engineering for Industry. 104(1):29–35

13. Koerber H, Xavier J, Camanho PP (2010) High strain rate characterisation of unidirectional carbon-epoxy IM7-8552 in transverse compression and in-plane shear using digital image correlation. Mech Mater 42(11):1004–1019. https://doi.org/10.1016/j.mechmat.2010.09.003

14. Kolsky H (1949) An investigation of the mechanical properties of material at very high rates of loading. Proc Phys Soc B 62(11):676–700

15. Lewis JL, Goldsmith W (1973) A biaxial split Hopkinson bar for simultaneous torsion and compression. Rev Sci Instrum 44(7):811–813. https://doi.org/10.1063/1.1686253

16. Liu T, Sun B, Gu B (2018) Size effects on compressive behaviors of three-dimensional braided composites under high strain rates. J Compos Mater 53(28):3895–3908. https://doi.org/10.1177/0021998318771459

17. Melin L, Asp L (1999) Effects of strain rate on transverse tension properties of a carbon/epoxy composite: Studied by moiré photography. Compos Part A Appl Sci Manuf 30(3):305–316. https://doi.org/10.1016/S1359-835X(98)00123-7

18. Muzychenko VP, Kashchenko SI, Guskov VA (1986) Application of the Hopkinson composite rod method in the study of the dynamic properties of materials (review). Head. Laboratory 1:58–66 (in Russ.)

19. Nicholas T (1981) Tensile testing of materials at high rates of strain. Exp Mech 21(5):177–195. https://doi.org/10.1007/BF02326644

20. Siviour CR, Jordan JL (2016) High strain rate mechanics of polymers: a review. J Dyn Behav Mater 2(1):15–32. https://doi.org/10.1007/s40870-016-0052-8

21. Zukas JA, Nicholas T, Swift H, Greszczuk LB, Curran DR (1982) Impact dynamics. New York. Chichester. Brisbane. Toronto. Singapore